

BROAD-LINED SUPERNOVA 2016COI WITH HELIUM ENVELOPE

MASAYUKI YAMANAKA¹, TATSUYA NAKAOKA², MASAOMI TANAKA³, KEIICHI MAEDA^{4,5}, SATOSHI HONDA⁶, HIDEKAZU HANAYAMA⁷, TOMOKI MOROKUMA⁸, MASATAKA IMAI⁹, KENZO KINUGASA¹⁰, KATSUHIRO L. MURATA¹¹, TAKEFUMI NISHIMORI¹², OSAMU HASHIMOTO¹³, HIROTAKA GIMA¹², KENSUKE HOSOYA⁶, AYANO ITO¹², MAYU KARITA⁶, MIHO KAWABATA², KUMIKO MORIHANA⁶, YUTO MORIKAWA¹², KOTONE MURAKAMI¹², TAKAHIRO NAGAYAMA¹², TATSUHARU ONO¹⁴, HIROKI ONOZATO¹⁵, YUKI SARUGAKU¹⁶, MITSUTERU SATO¹⁷, DAISUKE SUZUKI¹⁸, JUN TAKAHASHI⁶, MASAKI TAKAYAMA⁶, HIJIRI YAGUCHI⁶, HIROSHI AKITAYA^{2,19}, YUICHIRO ASAKURA²⁰, KOJI S. KAWABATA^{2,19}, DAISUKE KURODA²¹, DAISAKU NOGAMI⁴, YUMIKO OASA²², TOSHIHIRO OMODAKA¹², YOSHIHIKO SAITO²³, KAZUHIRO SEKIGUCHI³, NOZOMU TOMINAGA^{1,5}, MAKOTO UEMURA^{2,19}, AND MAKOTO WATANABE²⁴.

Draft version June 9, 2021

ABSTRACT

We present the early-phase spectra and the light curves of the broad-lined supernova (SN) 2016coi from $t = 7$ to 67 days after the estimated explosion date. This SN was initially reported as a broad-lined Type SN Ic (SN Ic-BL). However, we found that spectra up to $t = 12$ days exhibited the He I $\lambda 5876$, $\lambda 6678$, and $\lambda 7065$ absorption lines. We show that the smoothed and blueshifted spectra of normal SNe Ib are remarkably similar to the observed spectrum of SN 2016coi. The line velocities of SN 2016coi were similar to those of SNe Ic-BL and significantly faster than those of SNe Ib. Analyses of the line velocity and light curve suggest that the kinetic energy and the total ejecta mass of SN 2016coi are similar to those of SNe Ic-BL. Together with broad-lined SNe 2009bb and 2012ap for which the detection of He I were also reported, these SNe could be transitional objects between SNe Ic-BL and SNe Ib, and be classified as broad-lined Type ‘Ib’ SNe (SNe ‘Ib’-BL). Our work demonstrates the diversity of the outermost layer in broad-lined SNe, which should be related to the variety of the evolutionary paths.

Subject headings: supernovae: general — supernovae: individual (SN 2016coi) — supernovae: individual (SNe 1998bw, 2008D, 2009bb, 2012au)

¹ Department of Physics, Faculty of Science and Engineering, Konan University, Okamoto, Kobe, Hyogo 658-8501, Japan; yamanaka@center.konan-u.ac.jp

² Department of Physical Science, Hiroshima University, Kagamiyama 1-3-1, Higashi-Hiroshima 739-8526, Japan

³ National Astronomical Observatory of Japan, National Institutes of Natural Sciences, Osawa, Mitaka, Tokyo 181-8588, Japan

⁴ Department of Astronomy, Graduate School of Science, Kyoto University, Sakyo-ku, Kyoto 606-8502, Japan

⁵ Kavli Institute for the Physics and Mathematics of the Universe (WPI), The University of Tokyo, 5-1-5 Kashiwanoha, Kashiwa, Chiba 277-8583, Japan

⁶ Nishi-Harima Astronomical Observatory, Center for Astronomy, University of Hyogo, 407-2 Nishigaichi, Sayo-cho, Sayo, Hyogo 679-5313, Japan

⁷ Ishigakijima Astronomical Observatory, National Astronomical Observatory of Japan, National Institutes of Natural Sciences, 1024-1 Arakawa, Ishigaki, Okinawa 907-0024, Japan

⁸ Institute of Astronomy, Graduate School of Science, The University of Tokyo, 2-21-1 Osawa, Mitaka, Tokyo 181-0015, Japan

⁹ Department of CosmoSciences, Graduate School of Science, Hokkaido University, Kita 10 Nishi8, Kita-ku, Sapporo 060-0810, Japan

¹⁰ Nobeyama Radio Observatory, National Astronomical Observatory of Japan, National Institutes of Natural Sciences, 462-2 Nobeyama, Minamimaki, Minamisaku, Nagano 384-1305, Japan

¹¹ Department of Astrophysics, Nagoya University, Chikusa-ku, Nagoya 464-8602, Japan

¹² Graduate School of Science and Engineering, Kagoshima University, 1-21-35 Korimoto, Kagoshima 890-0065, Japan

¹³ Gunma Astronomical Observatory, Takayama, Gunma 377-0702, Japan

¹⁴ Earth and Planetary Sciences, School of Science, Hokkaido University, Kita 10 Nishi8, Kita-ku, Sapporo 060-0810, Japan

¹⁵ Astronomical Institute, Graduate School of Science, Tohoku University, 6-3 Aramaki Aoba, Aoba-ku, Sendai, Miyagi, 980-8578, Japan

¹⁶ Kiso Observatory, Institute of Astronomy, Graduate School of Science, The University of Tokyo, Mitake, Kiso-machi, Kiso, Nagano 397-0101, Japan

¹⁷ Faculty of Science, Hokkaido University, Kita 10 Nishi8, Kita-ku, Sapporo 060-0810, Japan

¹⁸ Code 667, NASA Goddard Space Flight Center, Greenbelt, MD 20771, USA

¹⁹ Hiroshima Astrophysical Science Center, Hiroshima University, Higashi-Hiroshima, Hiroshima 739-8526, Japan

²⁰ Institute for Space-Earth Environmental Research, Nagoya University, Furocho, Chikusa-ku, Nagoya, 464-8601, Japan

²¹ Okayama Astrophysical Observatory, National Astronomical Observatory of Japan, National Institutes of Natural Sciences, 3037-5 Honjo, Kamogata, Asakuchi, Okayama 719-0232, Japan

²² Faculty of Education, Saitama University, 255 Shimo-Ookubo, Sakura, Saitama, 338-8570, Japan

²³ Department of Physics, Tokyo Institute of Technology, 2-12-1 Ookayama, Meguro-ku, Tokyo 152-8551, Japan

²⁴ Department of Applied Physics, Okayama University of Science, 1-1, Ridai-cho, Kita-ku, Okayama, Okayama 700-0005, Japan

1. INTRODUCTION

Core collapse supernovae (SNe) are classified as Type Ib when the spectra exhibit the helium but not the hydrogen, while SNe are classified as Type Ic when the spectra exhibit neither helium nor hydrogen, (Filippenko 1997). The absorption lines reflect the compositions of the outer layers of the SN ejecta and progenitor. It is known that properties of SNe Ib/c have a large variety. Some SNe Ib/c show broad absorption features, and such objects are called broad-lined (BL) SN Ic (SN Ic-BL; Valenti et al. 2008). The high expansion velocities suggest that SNe Ic-BL have a higher energy than normal SNe Ib/c (Foley et al. 2003; Valenti et al. 2008). SNe Ic-BL associated with a γ -ray burst (GRB-SNe) forms a particularly missing subclass (Galama et al. 1998; Iwamoto et al. 1998). Their kinetic energy is likely to be even larger than those of other SNe Ic-BL (Nomoto et al. 2006). The origin of these varieties is, however, not well understood yet.

In theoretical stellar evolution models, it is not straightforward to produce SN progenitors with no He layer. Stellar wind and binary interaction play important roles in removing the envelope. Interestingly, even in the binary models, which is probably favored over single star models in removing the envelope, the progenitors tend to have some amount of helium layer (Woosley et al. 1995; Yoon et al. 2010; Yoon 2015). Thus, to study the evolutionary paths to GRB-SNe and SNe Ic-BL, it is important to observationally probe the presence of He in these classes of SNe.

Due to the relatively low event rate, the direct detection of the progenitor of SNe Ic-BL has never been reported to date. Thus, it is important to study the composition of the progenitor star from the early-phase spectra of SNe. In fact, the presence of the He features in optical and near-infrared (NIR) spectra of SNe Ic-BL has been suggested for SNe 2009bb and 2012ap (Pignata et al. 2011; Bufano et al. 2012; Milisavljevic et al. 2015). For SN 2009bb, the identification is, however, based mainly on the He I λ 5876 line, which could be contaminated by the Na I D line (Pignata et al. 2011). In the spectra of SN 2009bb, the He I λ 6678 and λ 7065 ones were very weak. For SN 2012ap, the strong He I λ 10830 line was detected, but the He I λ 20587 line, which is expected to have a similar strength to the He I λ 10830, was weak (Milisavljevic et al. 2015). Also, a statistic analysis of spectra of SNe Ic and SNe Ic-BL has been done by Modjaz et al. (2015). They reported that these types of SNe do not show detectable helium absorption lines. In sum, the presence of the He layer in SNe Ic and Ic-BL is still controversial.

In this paper, we present results of our observations of SN 2016coi. SN 2016coi was discovered at the outskirts of the nearby faint galaxy UGC 11868 on May 27.5 by ASAS-SN team (Holoien et al. 2016). The name of this SN was independently given as ASASSN-16fp. The distance of the host galaxy was obtained to be 17.2 Mpc using Tully-Fisher relation²⁵. Follow-up spectroscopic observations were performed by several groups and the spectra were very similar to those of SNe Ic-BL at their early phase (Elias-Rosa et al. 2016).

We first describe our observations and data reduction in §2. In §3, we compare the properties with those of SNe Ib and Ic-BL. We show that the spectral properties of SN 2016coi were very similar to those of SNe Ic-BL except for the detection of the He I absorption lines. This suggests that SN 2016coi is a transitional SN between SNe Ib and Ic-BL, and could be classified as an SN ‘Ib’-BL. Finally, we discuss the explosion properties and progenitor nature of SN 2016coi in §4.

2. OBSERVATIONS AND DATA REDUCTION

Observations of SN 2016coi were performed using various telescopes and instruments in the framework of the Target-of-Opportunity (ToO) program in the Optical and Infrared Synergetic Telescopes for Education and Research (OISTER). Optical spectroscopic observations were performed using the 1.5-m Kanata telescope attached with the Hiroshima One-shot Wide-field Polarimetry (HOWPol; Kawabata et al. 2008) on 14 nights from May 31 through Jul 4. Spectroscopic observations were also performed using the 1.5-m telescope attached with the Gunma LOW-resolution Spectrograph and imager (GLOWS) on three nights from Jun 2 through Jun 17, and the 2.0-m Nayuta telescope attached with the Medium And Low-dispersion Long-slit Spectrograph (MALLS) on four nights from Jun 2 through Jul 2.

Spectroscopic data were reduced according to the standard manner. Wavelength calibrations were performed for the HOWPol data using atmospheric lines observed in the same frame to the object, and for the GLOWS and the MALLS using the FeNeAr lamp. Flux calibrations were performed using the bright high-temperature standard stars. The atmospheric lines of the SN spectra were corrected for using the standard-star spectra.

Optical imaging observations were performed using the Kanata telescope attached with the HOWPol on 17 nights from May 31 through Jul 26, the 1.6-m Pirka telescope attached with the Multispectral Imager (MSI; Watanabe et al. 2012) on 21 nights from Jun 2 through Jul 25, the 1.05-m telescope attached with the Kiso Wide Field Camera (KWFC; Sako et al. 2012) on six nights from Jun 2 through Jun 17, and the 1.05-m telescope in the Multicolor Imaging Telescopes for Survey and Monstrous Explosions (MITSuME; Kotani et al. 2005) at the Ishigakijima Astronomical Observatory on 28 nights from Jun 3 through Jul 30. Imaging observations of photometric standard star fields were also performed using the HOWPol and the MSI on photometric nights. Near-infrared photometry were performed using the 1.4-m InfraRed Survey Facility (IRSF) telescope attached with the Simultaneous three-color InfraRed Imager for Unbiased Survey (SIRIUS; Nagayama et al. 2003) on Jun 3, the Kanata telescope attached with the Hiroshima Optical and Near-InfraRed camera (HONIR; Sakimoto et al. 2012; Akitaya et al. 2014; Ui et al. 2014) on Jun 1, the Nayuta telescope attached with Nishiharima Infrared Camera (NIC) on Jun 14, and the 1.0-m telescope at Kagoshima University on four nights from Jun 14 through Jul 21.

Reductions of the imaging data were performed in the similar methods to the previous studies (see Yamanaka et al. 2015, 2016b). The point spread function (PSF) photometry were performed using the *IRAF* software *DAOPHOT*. Standard magnitudes of the lo-

²⁵ The distance was taken from NASA/IPAC EXTRAGALACTIC DATABASE (NED), <https://ned.ipac.caltech.edu/>

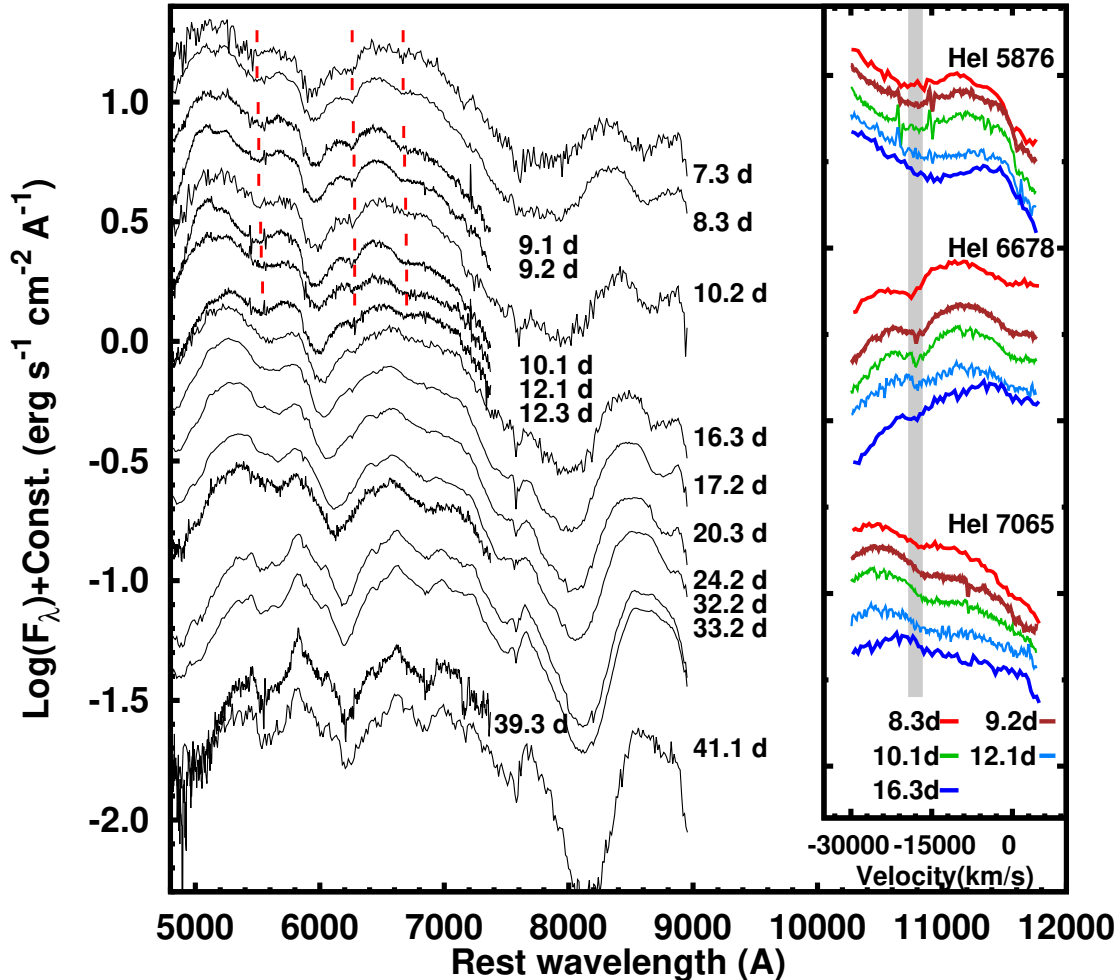


FIG. 1.— Spectral evolution of SN 2016coi from $t = 7$ to 41 d. Wavelengths of spectra were corrected for using the recession velocity of the host galaxy UGC 11868 ($z=0.0036$; Giovanelli & Haynes (1993)). Spectra were corrected for the atmospheric lines using the spectrophotometric standard star spectra. (Right inset) The close-up view of the He I $\lambda 5876$, $\lambda 6678$, and $\lambda 7065$ regions shown in the Doppler velocity. The vertical gray lines show the velocity of $18,000 \text{ km s}^{-1}$.

cal standard stars were obtained using the standard star magnitudes (Landolt 1992). Systematic differences among different instruments were confirmed. We corrected for the color terms of HOWPol (Kawabata et al. 2008), MSI (Watanabe et al. 2012), KWFC (Sako et al. 2012), and MITSuME (Kotani et al. 2005) when SN magnitudes were calculated. The color terms of these instruments were already obtained using the secondary standard stars in M67 (see also Yamanaka et al. 2015, 2016b). The systematic errors were calculated using the average of the residual differences.

The extinctions were corrected only for Galactic dust (Schlafly & Finkbeiner 2011). This is supported by the fact that the sodium absorption lines only from our Galaxy were detected in the spectra. The total extinction of $A_V = 0.2$ (Schlafly & Finkbeiner 2011) is adopted throughout this paper. The extinction coefficient is assumed to be $R_V = 3.1$ as a typical value.

3. RESULTS

3.1. Spectral features

Figure 1 shows the spectral evolution of SN 2016coi from $t = 7$ to 41 d²⁶. The corrected redshift is $z=0.0036$ for SN 2016coi. The spectra exhibited the strong absorption lines around 6000 \AA . The feature was identified as Si II $\lambda 6355$ and its velocity reached $18,000 \text{ km s}^{-1}$. The broad absorption line around at 8000 \AA was blended by the O I $\lambda 7774$ and Ca II IR triplet due to their extremely high velocities. Features marked by the red lines were attributed to He I. Identification of He I will be discussed in §3.2.

The spectrum at $t = 8 \text{ d}$ was compared with those of SNe Ic-BL 1998bw (Patat et al. 2001), 2002ap (Kawabata et al. 2002; Foley et al. 2003), and SN Ib 2008D (Modjaz et al. 2009) (see the top panel of Figure 2). The intensity of Si II $\lambda 6355$ absorption line of SN 2016coi was significantly stronger than those of other SNe. Although the absorption depth generally becomes shallower when the feature is broadened as seen in SN

²⁶ $t = 0$ is the estimated explosion date and defined as MJD 57532.5. See §3.3 for details.

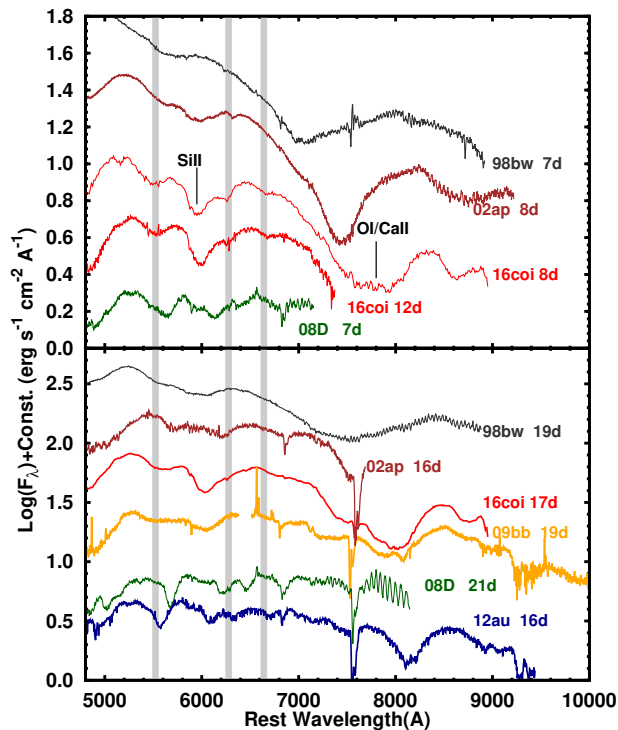


FIG. 2.— (Top panel) Spectra of SN 2016coi at $t = 8$ and 12 d compared with those of SNe Ic-BL 1998bw (Patat et al. 2001), 2002ap (Foley et al. 2003), and SN Ib 2008D (Modjaz et al. 2009). These data were taken from the SUSPECT^a and WIS-EREP^b databases. Vertical grey lines denote the wavelength the He I $\lambda 5876$, $\lambda 6678$, and $\lambda 7065$ which were blueshifted with $18,000 \text{ km s}^{-1}$. (Bottom panel) The spectrum at $t = 17$ d compared with those of other SNe as in the top panel as well as SNe 2009bb (Pignata et al. 2011) and 2012au (Takaki et al. 2013).

^a<https://www.nhn.ou.edu/suspect/>

^b<http://wiserep.weizmann.ac.il/>; (Yaron & Gal-Yam 2012)

1998bw, the absorption line of SN 2016coi was deep and broad.

The broad feature around $7400\text{--}8200 \text{ \AA}$ could not be separated into different lines. This characteristic is common in SNe Ic-BL. For SN 1998bw, the Ca II IR triplet was blueshifted to $\sim 7000 \text{ \AA}$ due to its extremely high-velocity ejecta and the feature was even blended with O I $\lambda 7774$ (Tanaka et al. 2007). For SN 2002ap, the feature was dominated by the O I only (Kawabata et al. 2002; Foley et al. 2003).

For the comparison of the spectrum at $t = 17$ d, the spectra of SN Ic-BL 2009bb (Pignata et al. 2011) and SN Ib 2012au (Takaki et al. 2013) were added (see the bottom panel of Figure 2). The line velocity of Si II $\lambda 6355$ was similar to those of SNe Ic-BL 1998bw and 2009bb (see also the middle panel of Figure 3), but significantly faster than those of SNe Ib 2008D and 2012au. The broad feature composed of the O I and Ca II lines was still seen at this epoch. This feature was also similar to those of SNe 1998bw and 2009bb. The same feature in SN 2012au was completely separated into the O I and Ca II. In summary, SN 2016coi is similar to an SN Ic-BL in many respects. However, as discussed below, the strong He I features were detected and the intensities were anomalously strong for SNe Ic-BL. With the spectra

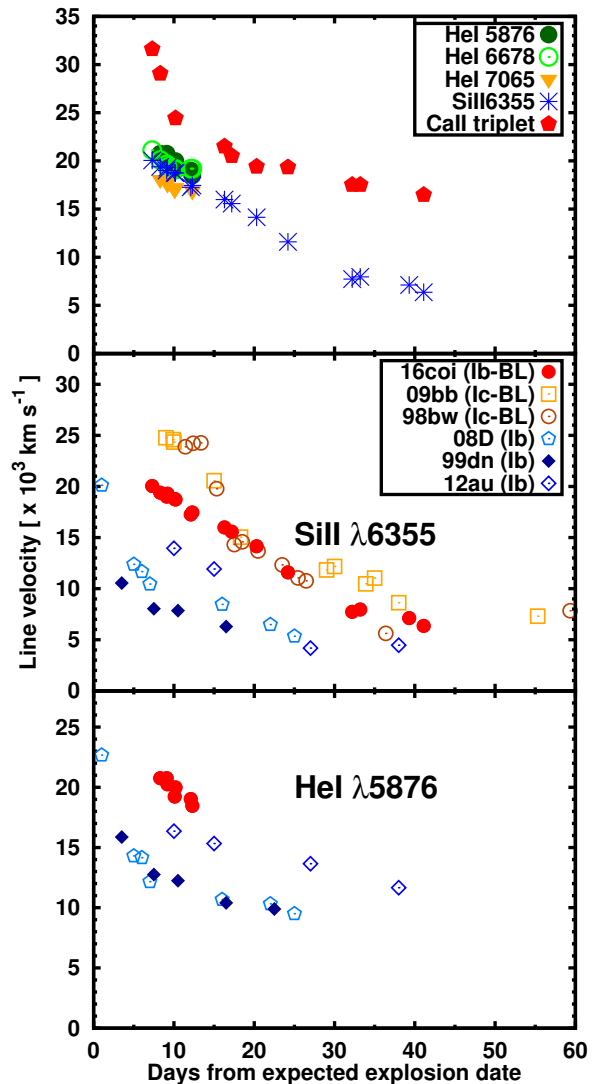


FIG. 3.— (Top panel) Velocity evolutions of Si II $\lambda 6355$, Ca II IR triplet, He I $\lambda 7065$, $\lambda 6678$, and $\lambda 5876$ lines. These line velocities were estimated from the absorption minimum measured using the *plot* task equipped with *IRAF*. (Middle panel) The line velocities of the Si II $\lambda 6355$ line compared with those of SNe Ic-BL 1998bw, 2009bb, SNe Ib 1999dn, 2008D, and 2012au. (Bottom panel) Similar to the middle panel, but for the He I $\lambda 5876$ line.

exhibiting He I, this SN should be classified as an SN ‘Ib’-BL according to the definition.

3.2. Detection of He I

Spectra up to $t = 12$ d exhibited the absorption lines at 5500 , 6300 , and 6850 \AA (see the inset of Figure 1). In this section, we show that these features were attributed to the absorption lines of He I $\lambda 5876$, $\lambda 6678$, and $\lambda 7065$. The velocities reached $18,000 \text{ km s}^{-1}$, and the corresponding wavelengths were denoted by the vertical gray lines in Figures 1 and 2.

In order to confirm the line identification of He I, we first produced artificially smoothed spectra of SN

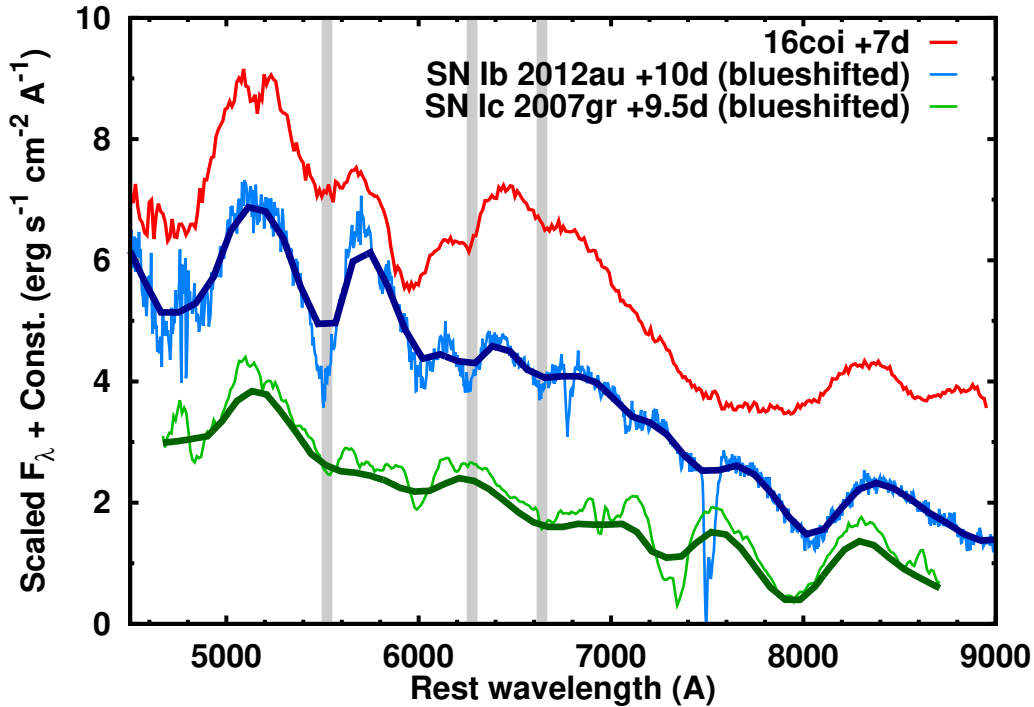


FIG. 4.— The spectrum of SN 2016coi at $t = 7$ d compared with the smoothed and blueshifted spectra of SN Ic 2007gr (Yamanaka et al. 2016a) and SN Ib 2012au. The flux intensity of these two SNe were artificially scaled for the comparison. The degree of blueshift is determined to match the He I absorption lines of SN 2016coi. Gaussian kernel smoothing were also performed for these two SNe to match the width of He I absorption lines of SN 2016coi. The vertical lines denote the He I absorption lines at their velocity of $18,000 \text{ km s}^{-1}$.

Ic 2007gr (Yamanaka et al. 2016a) and SN Ib 2012au (see Figure 4). We smoothed the spectra by using Gaussian kernel so that the Full-width-of-Half-Maximum (FWHM) of absorption lines of SN 2016coi ($11,000 \text{ km s}^{-1}$) matches to those of SNe 2007gr ($5,000 \text{ km s}^{-1}$) and 2012au ($7,500 \text{ km s}^{-1}$). Then, the spectra were further blueshifted to match the positions of the absorption lines. As shown in Figure 4, the spectrum of SN 2016coi was very similar to the smoothed and blueshifted spectrum of SN 2012au. We confirmed that in addition to the He I $\lambda 5876$ line, both the He I $\lambda 6678$ and $\lambda 7065$ features were similar in the spectrum of SN 2016coi and the smoothed and blueshifted spectrum of SN 2012au. On the other hand, as expected from Type Ic identification, the smoothed and blueshifted spectrum of SN 2007gr did not exhibit the He I absorption lines. These tests demonstrate that SN 2016coi show the He lines.

The relative absorption depths of the He lines were slightly different in SNe 2016coi and 2012au. We thus further study the possible He I features of SN 2016coi using the synthetic spectral code, SYN++ to assess possible contamination of the other lines in the He features. (Thomas et al. 2011). The O I, Na I, Si II, Si III, Ca II, Fe II, and Co II were used to reproduce the depth ratio. Figure 5 shows the Na ID and Si III features would contaminate to the broad line at 5600 \AA . The Co II $\lambda\lambda 5914, 6019$ help to explain the strength of the feature at 5600 \AA . The Co II $\lambda\lambda 6540, 6570$ also support to explain the strong absorption line at 6200 \AA (see Figure 5). The absorption lines at 5600 , 6200 and 6600 \AA were well explained using these components. On the other

hand, it is hard to explain the depth ratios without He I lines (see Figure 5).

Note that inclusion of Co II at 3800 \AA , 4400 \AA , and other elements is also consistent with a blue portion of the spectrum. Since Fe-group elements strongly affect the spectra in the ultraviolet wavelengths, we calculated $U - B$ color in the synthetic spectrum. The calculated color ($U - B = 0.6 \text{ mag}$) is consistent with observed $U - B$ within the error. The Mg II and Ti II features possibly contributes to the spectra below 4500 \AA , but again the U-band flux was consistent with the observed color even including these features.

To study the validity of our spectral fit, we also fit a spectrum of SN 2012au using the same ion species (He I, C I, O I, Na I, Si II, Si III, Ca II, Fe II, and Co II). The spectrum could be explained by the synthetic one except for slight differences at 6200 and 6600 \AA . The absorption features of He I were well matched. This suggests that the Co II features could support to improve the spectral fit.

In summary, we identified the He features in the pre-maximum spectra of SN 2016coi. The detection of the He lines has been suggested in other SNe Ic-BL. For SN Ic-BL 2009bb, the identification of He I has been discussed (Pignata et al. 2011). In SN 2009bb, the He I $\lambda 6678$ and He I $\lambda 7065$ features were very weak and the identification was marginal (see Figure 2). The near-infrared spectrum for SN 2012ap exhibited a strong absorption line around 10500 \AA (Milisavljevic et al. 2015). The NIR and optical features were simultaneously explained using the synthetic spectra, but they pointed out that the

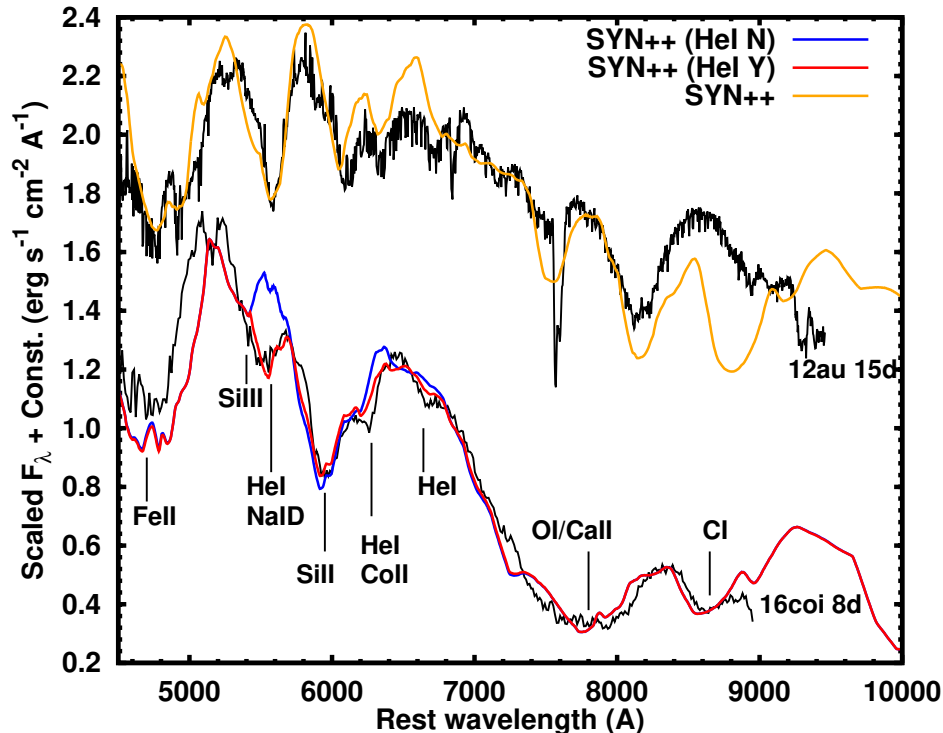


FIG. 5.— The observed spectrum of SN 2016coi at $t = 8$ d compared with the synthetic spectrum constructed using the SYN++ (Thomas et al. 2011). The He I, C I, O I, Na I, Si II, Si III, Ca II, Fe II and Co II features were used to calculate the spectrum. The synthetic spectrum without the only He I feature was also presented.

He λ 20587 feature was too weak to explain the strength of He λ 10830 (see also Bufano et al. 2012). Compared with these two previous cases, early-phase spectra of SN 2016coi gives more robust identification of the He I lines, because the lines were stronger than those of SN 2009bb and 2012ap.

The bottom panel of Figure 3 shows the comparison of the He λ 5876 line velocities with those of SNe Ib 1999dn (Benetti et al. 2011), 2008D, and 2012au. The He velocity of SN 2016coi was almost identical to that of Si λ 6355, and was the fastest among other SNe Ib until $t = 12$ d. Again, the Si λ 6355 line velocity of SN 2016coi was very similar to those of SNe 1998bw and 2009bb after $t = 15$ d. These facts support that SN 2016coi could be classified as an SN ‘Ib’-BL.

3.3. Light curves

Figure 6 shows the multi-band light curves of SN 2016coi. The V -band light curve showed the fast rise up in the first two data points. By extrapolating the rising part, the explosion date was estimated to be MJD 57532.5 (May 24.5). This is consistent with the upper-limit magnitude reported by Holoien et al. (2016), and this date is denoted to be $t = 0$ throughout this paper. The V -band light curves reached the maximum magnitude at $t = 17$ d.

The rising part of the light curves exhibited the slow evolution which was similar to those of SNe 1998bw, 2008D, and 2012au (see the upper panel of Figure 7). The estimated rise time of 17 days is almost similar to

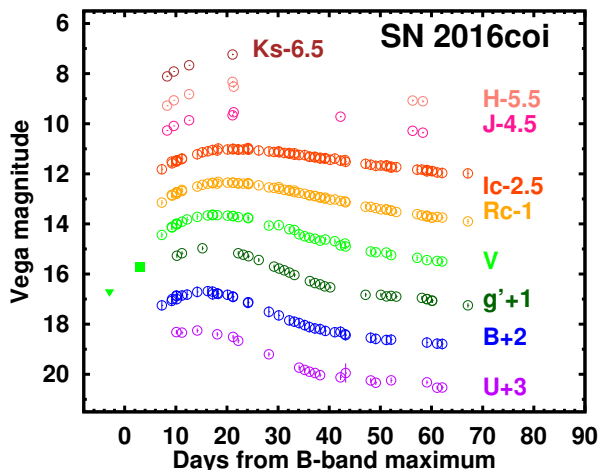


FIG. 6.— $UBg'VRIJHKs$ -band light curves of SN 2016coi. The explosion date was estimated to be MJD 57532.5 ($t = 0$) by extrapolating the rising part. The triangles denote the upper limit reported in Holoien et al. (2016).

16.5 days of SN 2012au and 18 days of SN 1998bw, and slightly shorter than that of SN 2009bb. SN 2008D has a longer rise time than that of SN 2016coi. The decline rate of SN 2016coi was also similar to those of SNe 1998bw, 1999dn, 2008D, and 2012au, but significantly slower than those of SNe 1994I and 2009bb.

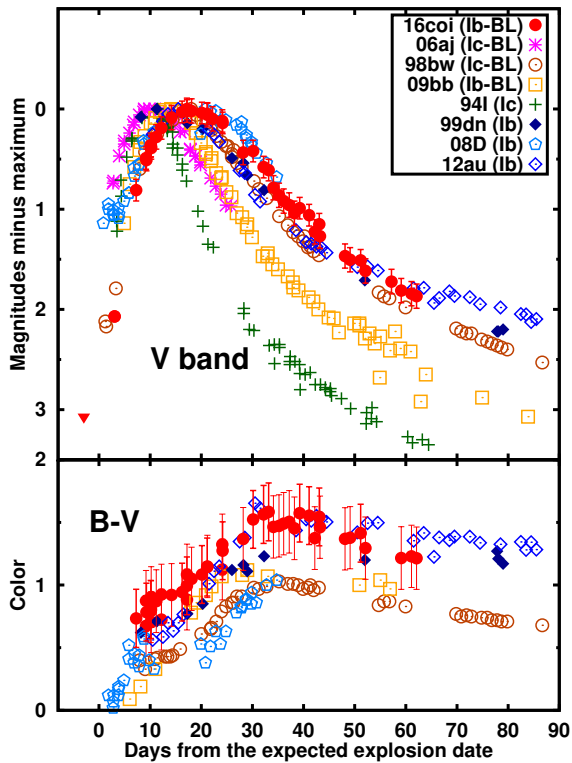


FIG. 7.— (Top panel) The V-band light curve compared with those of SNe Ic-BL 1998bw (Clocchiatti et al. 2011), 2006aj (Ferrero et al. 2006), 2009bb (Pignata et al. 2011), a normal SN Ic 1994I (Richmond et al. 1996), SNe Ib 2008D (Modjaz et al. 2009), and 2012au (Takaki et al. 2013). The light curves are shown in the magnitudes relative to the maximum. (Bottom panel) The $B - V$ color evolution compared with those of other SNe as in the top panel. Color excesses due to the Galactic and host galactic extinction were corrected for using the reported values in each reference.

The bottom panel of Figure 7 shows $B - V$ color evolution. The color excesses were corrected for using the values reported in each reference. The $B - V$ evolution of SN 2016coi was very similar to those of SNe 1999dn and 2012au, but different from that of SNe 1998bw, 2008D, and 2009bb. The color was always redder than those of SNe Ic-BL, and rather similar to those of SNe Ib.

To derive the absolute bolometric luminosity of SN 2016coi, the integration of the multi-band light curve was performed. The contribution of the optical emission to the total bolometric luminosity around the maximum date was assumed to be 60%. The distance modulus of $\mu = 31.18$ mag was adopted, which was taken from *NED*. For the comparison, the quasi-bolometric light curves of SNe 1998bw, 1999dn, 2008D, 2009bb and 2012au were also constructed in the same manner. Figure 8 shows the quasi-bolometric light curves of these SNe.

The peak luminosity of SN 2016coi was estimated to be 3.2×10^{42} erg s^{-1} . It was substantially fainter than those of SNe 1998bw, 2009bb and 2012au. It was more luminous than those of SNe 1999dn and 2008D. The ^{56}Ni mass of SN 2016coi was estimated to be $\sim 0.15M_{\odot}$ as-

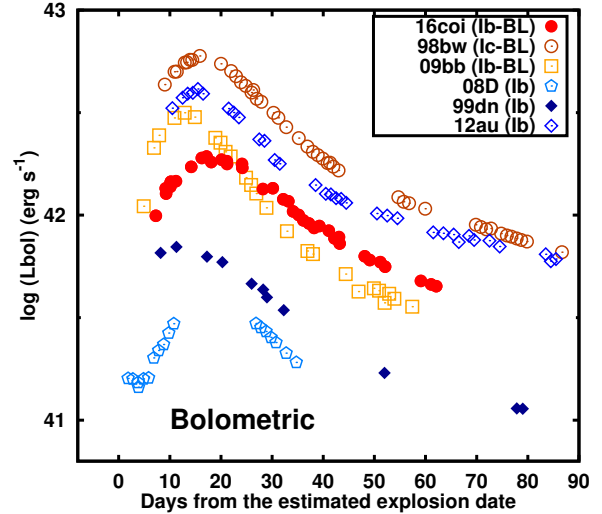


FIG. 8.— Quasi-bolometric light curve compared with those of other SNe. The bolometric light curves were constructed using optical (BVR I-band) light curves assuming that the optical fluxes are 60% to the total luminosity.

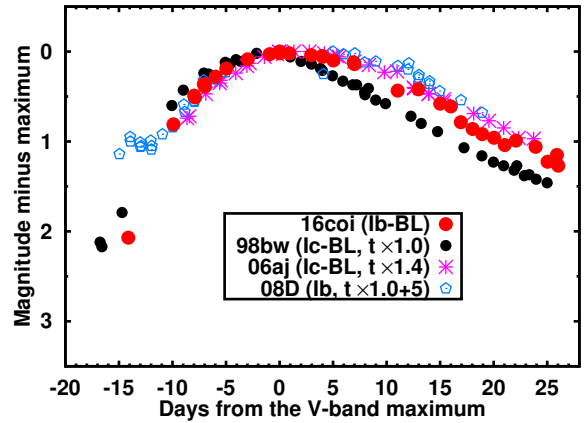


FIG. 9.— The V-band light curves compared with the stretched and shifted light curves of SNe 1998bw, 2006aj, and 2008D.

suming that the rise time was 17 days and $\alpha = 1$ (Arnett 1982; Stritzinger & Leibundgut 2005). This ^{56}Ni mass was relatively small among SNe Ic-BL, while it is more consistent with normal SNe Ib.

4. DISCUSSION AND CONCLUSION

In this paper, we showed results of our photometric and spectroscopic observations of SN 2016coi. The He I lines were clearly identified in the spectra. Except for the presence of He I, the spectral features of SN 2016coi were similar to those of SNe Ic-BL. The line velocity as well as broad features of Si II and Ca II absorption lines were also similar to SNe Ic-BL. Pignata et al. (2011) pointed out that the He I features were detected in spectra of SN Ic-BL 2009bb. The detection of the possible He I features in NIR spectra were also reported for SN 2012ap (Milisavljevic et al. 2015). The detection of the helium

in these SNe means that these are classified as SNe Ib according to the definition. We suggest the classification of these SN to be ‘Ib’-BL.

We estimate the kinetic energy and the total ejecta mass of SN 2016coi using the scaling method (see Sahu et al. 2008). Since the light curve shape of SN 2016coi was similar to the stretched light curve of SNe 2006aj and 2008D (see Figure 9), we use these objects as references. The light curve timescale of SN 2016coi was 1.4 times longer than that of SN 2006aj while it is comparable to that of SN 2008D. The Si II line velocity of $\sim 15,000 \text{ km s}^{-1}$ was similar to of SN 2006aj and 1.6 times larger than the 9000 km s^{-1} of SN 2008D. Thus, by using SN 2006aj as a reference (Mazzali et al. 2006), the total ejected mass and the kinetic energy were estimated to be $M_{ej} \sim 10M_{\odot}$ and $E_k \sim 3.0 \times 10^{52} \text{ erg}$. Similarly, by using SN 2008D as a reference (Tanaka et al. 2009), the kinetic energy and the total ejected mass were estimated to be $M_{ej} \sim 10M_{\odot}$ and $E_k \sim 5.0 \times 10^{52} \text{ erg}$. The estimated ejecta masses and the kinetic energies were similar to those of GRB-SNe.

The presence of He in other broad-lined SNe is of great interest. To study this possibility, we further smoothed and blueshifted spectrum of SN 2016coi to match the absorption velocity and width to those of SN 1998bw (see Figure 10). We confirmed that smoothed spectrum of SN 2016coi still shows a hint of the He I features while it is not seen in the spectrum of SN 1998bw. Therefore, SN 1998bw does not have a similar amount of He. These considerations suggest that SNe 2016coi (also SNe 2009bb and 2012ap) may belong to a different class of SNe from the prototype of broad-lined SNe. This is in line with the finding by Modjaz et al. (2015), who concluded that SNe Ic-BL are He free. There may be diversity among broad-lined SNe in terms of helium contents in the outer layer. A caveat is that it would also be possible that other broad-lined SNe still contain the He layer, but the He lines are not strong in absence of the non-thermal excitation (e.g., Hachinger et al. 2012).

This work demonstrates an important role of very early phase observations for the identification of He in broad-lined SNe. The He I absorption lines seen in SN 2016coi became very weak at $t = 15 \text{ d}$, while the He I lines generally become stronger at the later epoch for SNe Ib

(Matheson et al. 2001). We speculate that the He I lines may have eluded the detection due to the lack of pre-maximum early phase spectra.

Our work demonstrated a diversity of the outermost layer in broad-lined SNe. The presence of He in broad-lined SNe is indeed in favor of standard stellar evolution models as it is difficult to remove all the helium layer from the progenitor in many models (Woosley et al. 1995; Yoon et al. 2010; Yoon 2015). The observed diversity must reflect the variety of the evolutionary paths, but the exact origin is not yet understood. To understand the evolutionary paths to broad-lined SNe and their variety, observations of more broad-lined SNe from early phases will be important.

This work was supported by the Optical and Near-infrared Astronomy Inter-University Cooperation Program, and the Hirao Taro Foundation of the Konan University Association for Academic Research. This work

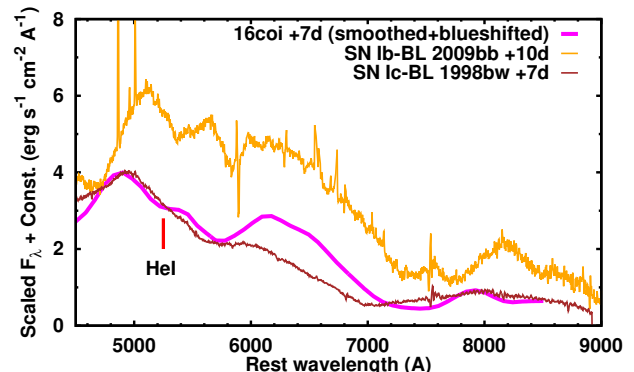


FIG. 10.— Blueshifted and smoothed spectrum of SN 2016coi compared with spectra of SNe Ic-BL 1998bw and 2009bb. The He I $\lambda 5876$ feature was seen in SN 2016coi, but not in SN 1998bw.

was partly supported by the Grant-in-Aid for Scientific Research from JSPS (26800100, 15H02075, 15H00788). The work by K.M. is partly supported by WPI Initiative, Mext, Japan.

REFERENCES

- Akitaya, H., et al. 2014, in Proc. SPIE, Vol. 9147, Ground-based and Airborne Instrumentation for Astronomy V, 91474O
- Arnett, W. D. 1982, ApJ, 253, 785
- Benetti, S., et al. 2011, MNRAS, 411, 2726
- Bufano, F., et al. 2012, ApJ, 753, 67
- Clocchiatti, A., Suntzeff, N. B., Covarrubias, R., & Candia, P. 2011, AJ, 141, 163
- Elias-Rosa, N., et al. 2016, The Astronomer’s Telegram, 9090
- Ferrero, P., et al. 2006, A&A, 457, 857
- Filippenko, A. V. 1997, ARA&A, 35, 309
- Foley, R. J., et al. 2003, PASP, 115, 1220
- Galama, T. J., et al. 1998, Nature, 395, 670
- Giovanelli, R., & Haynes, M. P. 1993, AJ, 105, 1271
- Hachinger, S., Mazzali, P. A., Taubenberger, S., Hillebrandt, W., Nomoto, K., & Sauer, D. N. 2012, MNRAS, 422, 70
- Holoien, T. W.-S., et al. 2016, The Astronomer’s Telegram, 9086
- Iwamoto, K., et al. 1998, Nature, 395, 672
- Kawabata, K. S., et al. 2002, ApJ, 580, L39
- Kawabata, K. S., et al. 2008, in Society of Photo-Optical Instrumentation Engineers (SPIE) Conference Series, Vol. 7014, Society of Photo-Optical Instrumentation Engineers (SPIE) Conference Series
- Kotani, T., et al. 2005, Nuovo Cimento C Geophysics Space Physics C, 28, 755
- Landolt, A. U. 1992, AJ, 104, 340
- Matheson, T., Filippenko, A. V., Li, W., Leonard, D. C., & Shields, J. C. 2001, AJ, 121, 1648
- Mazzali, P. A., et al. 2006, Nature, 442, 1018
- Milisavljevic, D., et al. 2015, ApJ, 799, 51
- Modjaz, M., Liu, Y. Q., Bianco, F. B., & Graur, O. 2015, ArXiv e-prints
- Modjaz, M., et al. 2009, ApJ, 702, 226
- Nagayama, T., et al. 2003, in Society of Photo-Optical Instrumentation Engineers (SPIE) Conference Series, Vol. 4841, Instrument Design and Performance for Optical/Infrared Ground-based Telescopes, ed. M. Iye & A. F. M. Moorwood, 459–464
- Nomoto, K., Tominaga, N., Umeda, H., Kobayashi, C., & Maeda, K. 2006, Nuclear Physics A, 777, 424
- Patat, F., et al. 2001, ApJ, 555, 900
- Pignata, G., et al. 2011, ApJ, 728, 14
- Richmond, M. W., et al. 1996, AJ, 111, 327
- Sahu, D. K., et al. 2008, ApJ, 680, 580
- Sakimoto, K., et al. 2012, in Proc. SPIE, Vol. 8446, Ground-based and Airborne Instrumentation for Astronomy IV, 844673
- Sako, S., et al. 2012, in Proc. SPIE, Vol. 8446, Ground-based and Airborne Instrumentation for Astronomy IV, 84466L
- Schlafly, E. F., & Finkbeiner, D. P. 2011, ApJ, 737, 103

- Stritzinger, M., & Leibundgut, B. 2005, *A&A*, 431, 423
- Takaki, K., et al. 2013, *ApJ*, 772, L17
- Tanaka, M., Maeda, K., Mazzali, P. A., & Nomoto, K. 2007, *ApJ*, 668, L19
- Tanaka, M., et al. 2009, *ApJ*, 692, 1131
- Thomas, R. C., Nugent, P. E., & Meza, J. C. 2011, *PASP*, 123, 237
- Ui, T., et al. 2014, in *Proc. SPIE*, Vol. 9147, Ground-based and Airborne Instrumentation for Astronomy V, 91476C
- Valenti, S., et al. 2008, *MNRAS*, 383, 1485
- Watanabe, M., Takahashi, Y., Sato, M., Watanabe, S., Fukuhara, T., Hamamoto, K., & Ozaki, A. 2012, in *Proc. SPIE*, Vol. 8446, Ground-based and Airborne Instrumentation for Astronomy IV, 84462O
- Woosley, S. E., Langer, N., & Weaver, T. A. 1995, *ApJ*, 448, 315
- Yamanaka, M., et al. 2015, *ApJ*, 806, 191
- . 2016a, et al. submitted to *PASJ*
- . 2016b, ArXiv e-prints
- Yaron, O., & Gal-Yam, A. 2012, *PASP*, 124, 668
- Yoon, S.-C. 2015, *PASA*, 32, e015
- Yoon, S.-C., Woosley, S. E., & Langer, N. 2010, *ApJ*, 725, 940